

**Paper 30-1** has been designated as a Distinguished Paper at Display Week 2025. The full-length version of this paper appears in a Special Section of the *Journal of the Society for Information Display (JSID)* devoted to Display Week 2025 Distinguished Papers. This Special Section will be freely accessible until December 31, 2025 via:

<https://sid.onlinelibrary.wiley.com/doi/full/10.1002/jsid.2060>

Authors that wish to refer to this work are advised to cite the full-length version by referring to its DOI:

<https://doi.org/10.1002/jsid.2060>



# Measuring and Characterizing the Diffractive Component in Display Reflection

Ingo Rotscholl, Kilian Kirchhoff, Alexander Voelz, Udo Krüger

TechnoTeam Bildverarbeitung GmbH, Ilmenau, Germany

Contact: [ingo.rotscholl@technoteam.de](mailto:ingo.rotscholl@technoteam.de)

## Abstract

We present and validate an easy-to-setup approach to measure the reflection properties of a display that can measure not only the specular, haze, and Lambertian components of display reflection, but also the diffractive component. We then research the fundamental dependencies of this fourth reflection component through a series of measurements using a variable aperture source.

## Author Keywords

Display metrology, Imaging Luminance Measurement Device, Reflection, Variable aperture source, Diffraction

## 1. Introduction

Display performance under ambient lighting conditions is important for many applications because most displays interact with ambient light. While reflective displays require ambient light, emissive displays usually compete with it. A poor ambient light performance can be disturbing – for instance, at home when watching TV– or downright dangerous, for example when a car display distracts the driver's attention too long because the content is difficult to read.

Therefore, characterizing display reflections and a solid understanding of each display's specific characteristics are important during the development or validation of high-quality displays. Here, the characterization and modeling of display diffraction plays an important role [1].

The first part of this paper briefly summarizes a recently published imaging-based reflection measurement method, that uses an Imaging Luminance Measurement Device (ILMD) with type 2 calibration [2] and a conoscopic lens to capture multiple viewing directions from a small area in one shot. Penzcek showed previously that ILMDs yield similar results as spot-meters for established reflection measurement methods [3]. In this paper, we now focus on validating the specific one-shot conoscopic imaging and alignment method by comparing it to high-resolution ILMD-based reflection measurements.

After that, we will use our validated method to investigate the diffractive component of reflections, which has often been neglected in previous research. We characterize its fundamental dependencies regarding the light source through several measurement series using a variable aperture source. Finally, we will provide a summary and outlook of future works regarding the diffractive component.

## 2. State of the art

According to Kelley, the reflected luminance of a display is the sum of three different components [4]. The first one is the reflected Lambertian component  $L_{Lamb}$ . The second component is the reflected haze component  $L_{Haze}$  and the third one is the reflected specular component  $L_{Spec}$  according to Eq. 1. Figure 1 provides an image of a 2D reflection characteristic and a luminance projection of a typical reflection where these three

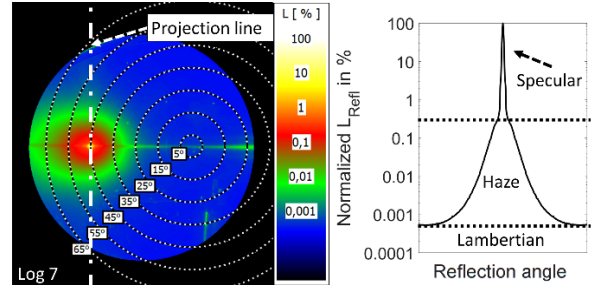


**Figure 1: Exemplary luminance reflection characteristic as a 2D plot and 1-D projection visualizing its components. The angle of incidence is  $\theta_s = 45^\circ$  and  $\phi_s = 0^\circ$**

components occur. Each ILMD pixel in this image and along the projection corresponds to a different viewing angle ( $\theta_d, \phi_d$ ).

Each component has different dependencies regarding the ambient illumination. While the specular component is a mirror-like reflection and thus a function of the light source Luminance  $L_S$ , the Lambertian component is only a function of the Illuminance  $E$  on the display surface. The haze component, which is centered around the specular peak, is often the most critical among these three in practical applications and depends on  $E$  and the angular subtense  $\Psi_S$  of the light source. Thus the total amount of reflected luminance  $L_{Refl}$ , is given as [5,6]:

$$L_{Refl} = L_{Lamb} + L_{Haze} + L_{Spec} \quad (1)$$

$$L_{Refl} = \frac{\rho}{\pi} E + \frac{R_{Haze}(\Psi_S)}{\pi} E + \xi L_S$$

To model the reflection properties with respect to different ambient light sources, the separation of these components is required. This can for instance be done with the variable aperture source (VAS) and annulus source method [6]. Here, a light source with well-defined and changeable apertures is used in a measurement series. Additionally, the light source has a small annulus in the center. Thus, the specular component can be excluded locally, which allows the precise measurement of  $\xi$ . The Lambertian reflectance factor  $\rho$  can be separated by measuring the reflected luminance with the detector placed at an angle far away from the specular peak and the haze component, where it is assumed that only Lambertian reflection occurs. A typical measurement geometry for this is 45/0. This means that the light source incidence  $\theta_s$  is  $45^\circ$  relative to the display normal with the measurement angle  $\theta_d = 0^\circ$  i.e. equal to the display normal. The terminology assumes a constant  $\phi$  plane.

## 3. The diffractive component

However, not much attention has been paid to another component that can occur in display reflection – the diffractive luminance component  $L_{Diff}$ . This is the part of the luminance reflection that is diffracted by the periodic structures of the display. It originates from the specular peak and can be strongly localized in both

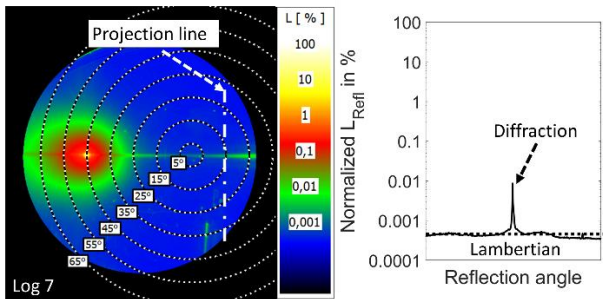


Figure 2: Exemplarily luminance reflection as 2D plot visualizing the diffractive component. The angle of incidence is  $\theta_s = 45^\circ$  and  $\phi_s = 0^\circ$

direction and spectrum. This results in gradients and sometimes colorful structures in different viewing directions  $(\theta_d, \phi_d)$ . The example in Figure 2 shows a diffraction, which occurs at  $\phi_d = 0^\circ$  in the 2D distribution, and also a Lambertian projection where the diffraction is dominant against the Lambertian component.

As diffractive effects are not part of the conventional three-component model, we extend Kelley's original model by the diffractive component  $L_{Diff}$ , which gives a four component model:

$$L_{Refl} = L_{Lamb} + L_{Haze} + L_{Spec} + L_{Diff} \quad (2)$$

With spot-meter based measurements, these diffractive structures are hard to measure, due to strong gradients and small structure sizes, as well as the unknown directions in both  $\theta_d$  and  $\phi_d$ . Thus, there can be no "standard" geometry (like 45/0) where all displays will always exhibit diffraction. Figure 3 shows four different reflection distributions with different directions of diffractive components. In all four cases the angle of incidence was  $45^\circ$  with  $\Psi_s = 0.5^\circ$ . A scanning method using a goniometer could reduce the second problem but increases measurement time and setup complexity as specialized mechanics are required.

ILMD-based reflection measurements, on the other hand, can not only determine the existence of a significant diffraction component and its corresponding directions, but are also capable to do that with higher resolution in less time. However, a lens-related trade-off exists between the measurement field angle and the angular resolution of the ILMD. A wide field of view lens can capture more directions in one shot. In contrast, a longer focal length with a narrower field of view will resolve more details. A scanning procedure, e.g., with a goniometer can again overcome this limitation but still leads to a more complex setup.

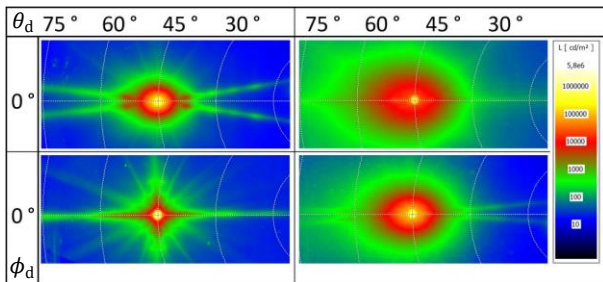


Figure 3: Reflection distribution for four different DUTs (same reflection geometry and light source), which all exhibit significant different diffraction in terms of intensity and direction

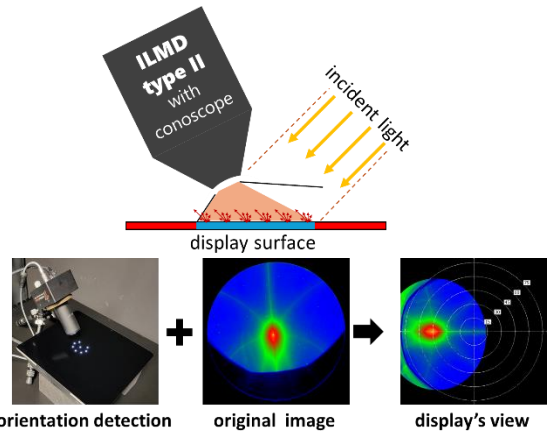


Figure 4: Conoscopic approach with orientation detection and transformation to the DUT standard view

#### 4. Conoscopic approach and its validation

In [7] we introduced a conoscopic reflection measurement approach that can capture many viewing directions in one shot. This provides a quick overview of the whole reflected luminance distribution, as shown in Fig. 1 and 2. The general concept is illustrated in Figure 4. A wide field of view conoscopic lens is placed close to the DUT surface capturing the reflected light rays from an extended but rather small measurement surface. Based on a specific display test pattern, the specific orientation of the ILMD type II relative to the display surface is detected. That information is used to assign the measured luminance data to the display's polar coordinate system  $(\theta_d, \phi_d)$ , such that each point in an image corresponds to a viewing direction of the display. In addition, photometric corrections using e.g., a calibrated reflection target, are required to assess the potentially non-uniform illuminance across the measured area. More details are provided in [7]. The method was validated for reproducibility regarding an ISO 15008 conformity analysis in a round-robin experiment. However, unlike for the evaluation and separation of different display reflection components, the ISO 15008 analysis did not require a high angular resolution or precise data of the specular component.

To validate the one-shot conoscopic reflection measurement approach regarding its capability to separate the display reflection components, we compare it to high-resolution (HR) ILMD-based measurements. We extract the specular and Lambertian components from a typically used 15/15 (specular) geometry using a  $1^\circ$  angular subtense  $\Psi_s$  with a  $0.3^\circ$  annulus and a 45/0 geometry (Lambertian) with a  $\Psi_s$  of  $15^\circ$  with both lenses according to the annulus source method [5, 6]. As samples we use a reflective display with and without a specular cover glass and a glossy emissive display with and without a matt cover glass similar to the samples in the original papers [5] in black and white state. As the evaluation principle is the same as in [5,6], the experiment validates the conoscopic detection orientation and the imaging conditions of the conoscopic lens.

The geometry of the HR lens reference measurement is provided in Figure 5. We use two different LMK 6-12 cameras as ILMDs. One is equipped with a conoscopic lens with an angular resolution  $0.05^\circ/\text{cpx}$  (degree per camera pixel) with a total field of view of  $120^\circ$  circular. The second LMK was equipped with a high-resolution 100 mm lens that had an angular resolution of  $0.002^\circ/\text{cpx}$  with a total field of view of  $8.6^\circ \times 6.34^\circ$ . As light source we used an ISMS-30-VAS from Gigahertz Optik.

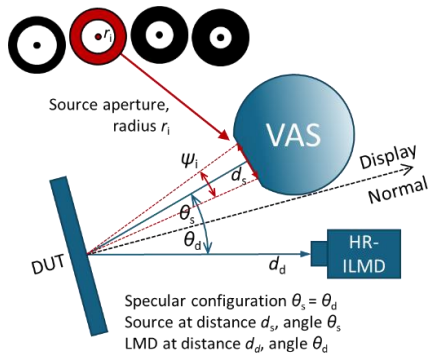


**Figure 5: Reference setup of the HR lens measurement (specular configuration), image modified from [6]**

Table 1 shows the derived specular and Lambertian reflection coefficients for the black and white state respectively for all samples. The four displays show specular and Lambertian reflection factors in different orders of magnitude but always similar values for both setups. The relative deviations increase with decreasing reflection factors but generally we consider the results of the conoscopic results valid enough to proceed to use it for analyzing the diffractive component.

**5. Experiments**

Our goal is to experimentally assess how the three light source parameters,  $L_S$ ,  $E$  and  $\Psi_S$  influence the diffractive reflection component, for a specific geometry and constant light source spectrum. The measurements are preformed using our conoscopic approach as introduced in the previous section. As light source, we use our ISMS-30-VAS with 4 different apertures.

We can only keep one of the three light source parameters constant because if we kept two parameters constant, the third one would also remain constant. Consequently, we identified four options. First, we can dim the light source, which changes  $L_S$  and  $E$  by the same factor, while  $\Psi_S$  remains constant.

**Table 1: Comparison of conoscopic and HR setup using the variable annulus source method**

DUT	Display color	Component	Result	
			HR lens	Conoscope
Glossy native	White	$\rho$	0.0019	0.0018
		$\xi$	0.0127	0.0135
	Black	$\rho$	0.0013	0.0011
		$\xi$	0.0127	0.0136
Glossy cover	White	$\rho$	0.0043	0.0032
		$\xi$	0.0017	0.0015
	Black	$\rho$	0.0039	0.0036
		$\xi$	0.0017	0.0015
Reflective native	White	$\rho$	0.4255	0.4390
		$\xi$	0.0002	0.0001
	Black	$\rho$	0.0323	0.0360
		$\xi$	0.0002	0.0001
Reflective cover	White	$\rho$	0.4102	0.4180
		$\xi$	0.0563	0.0572
	Black	$\rho$	0.0289	0.0320
		$\xi$	0.0565	0.0578

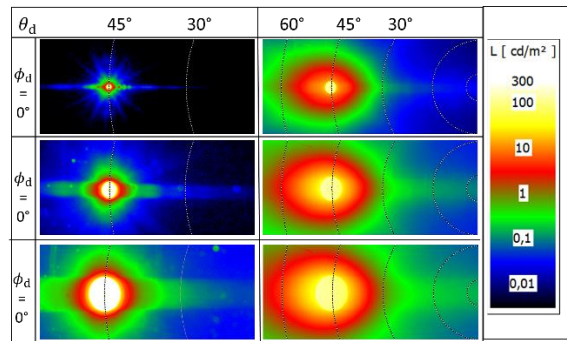


**Figure 6: Conoscopic luminance images for different illumination conditions: Left: LCD, Right: OLED**

However, we do not see any value in this option. Second, we can change the distance between DUT and VAS with a constant aperture. Then we effectively change  $E$  and  $\Psi_S$ , while  $L_S$  remains constant. And finally, we can change the aperture and adjust the distance. We can either try to achieve an approximately constant illuminance  $E$ , while  $\Psi_S$  and  $L_S$  are changed or we can keep  $\Psi_S$  constant while  $E$  and  $L_S$  are changed. We thus performed measurements which either have a constant  $L_S$ , an approximately constant  $E$  or a approximately constant  $\Psi_S$ . The last two series could only be achieved with the three larger apertures.

We measured the 2D distribution for two glossy emissive displays — one LCD and one OLED. Exemplary luminance images zoomed to the specular peak are shown in Figure 6. The angle of incidence is  $\theta_s = 45^\circ$  and  $\phi_s = 0$  in all measurements.

**6. Analyzing the diffractive component**

Although we measure 2D distributions, we now only evaluate the reflected luminance  $L_{Ref}$  as projection data similar to the plots shown in Fig 2. We select the evaluation region such that  $L_{Ref}$  does not contain any significant contribution from the specular component or its haze but the proposed  $L_{Diff}$  is prominent. Under these special conditions, we need only to correct for the approx. constant Lambertian component, which depends on  $\rho$  and  $E$

$$L_{Diff} = L_{Ref} - \frac{\rho}{\pi} E \tag{3}$$

To get a statistically robust  $L_{Ref}$  value, we calculate the 99% percentile in the evaluation area, which is more robust against outliers than the actual maximum.

Figure 7 shows how  $L_{Diff}$  according to Eq. 3 changes with the ambient lighting conditions for constant  $L_S$  measurements. But the increasing  $L_{Diff}$  could either be explained the variable  $E$ ,  $\Psi_S$  or a combination of both. But if it would be a pure  $E$  dependency,  $L_{Diff}$  could be explained by a factor similar to  $\rho$ . This is not the case. Thus, we conclude there is at least a  $\Psi_S$  dependency.

Figure 8 (top) shows  $L_{Diff}$  as a function of  $L_S$  for measurements with constant  $E$ . It appears that  $L_S \propto L_{Diff}$  for both displays. However, a significant, illogical offset occurs if we linearly extrapolate the data to zero (a switched-off light source). One reason for the offset error is that we did not correct for the different  $\Psi_S$ , that impacts  $L_{Diff}$  in to the constant  $L_S$  measurements (Figure 7). Furthermore, as  $E$  is constant, it cannot be the origin of the extrapolated offset error.

We now assume that the data from the constant  $L_S$  measurement can be explained by a pure  $\Psi_S$  dependency. Thus, we piecewise linearly interpolate a  $\Psi_S$  - correction factor. Using this factor, we can correct for the fact that  $\Psi_S$  unavoidably varied across different

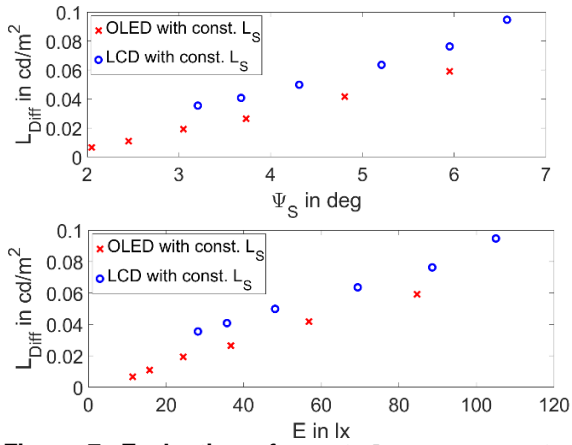


**Figure 7: Evaluation of const.  $L$  measurements: Top  $L_{Diff}$  as a function of  $\Psi_S$  and bottom as a function of  $E$**

data points from the const.  $E$  measurements. After applying this correction, we see a reasonable linear dependency, which has no strong offset for a switched-off light source (Figure 8 bottom).

In addition, we performed constant  $\Psi_S$  measurements to check our  $\Psi_S$  correction data. These data points match those of the  $\Psi_S$  correction very well (see Fig. 8) and validate our assumption that  $L_{Diff}$  scales linearly with  $L_S$  and that there is no  $E$ . dependency

$$L_{Diff} = R_{Diff}(\Psi_S)L_S \quad (4)$$

This relation can also be explained. A linear  $L_S$  dependency means that the light ray's angle of incidence determines the diffraction intensity and direction ( $\theta_d, \phi_d$ ). A strong illuminance linearity in contrast would mean that the diffractive component shows a similar behavior for a given viewing angle ( $\theta_d, \phi_d$ ) independent on the angle of incidence of the light ray. However, for diffraction, this would be unexpected.

The dependency of  $L_{Diff}$  on the light source subtense  $\Psi_S$  can be explained by an additive model, in which the angularly extended light source is decomposed into many infinitesimal small light sources with a small angular displacement. Each of these point-like light sources creates a diffraction profile. These slightly displaced diffraction profiles now overlap, e.g., due to scattering or the diffraction itself. That is very similar to the haze component model and also explains the blurring of the diffraction structures for larger angular subtenses (see Figure 6).

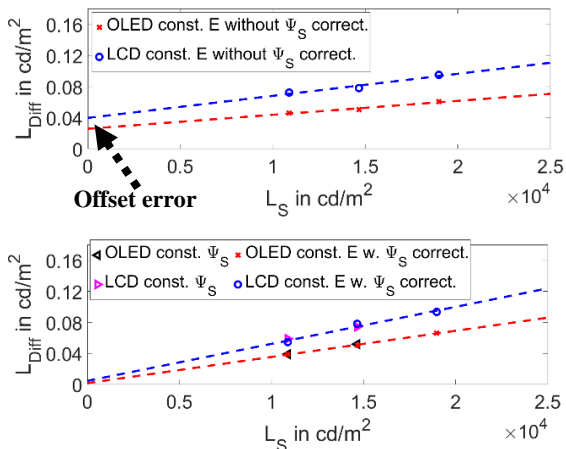


**Figure 8: Evaluation of const.  $E$  and  $\Psi_S$  measurements: Top: const.  $E$ , Bottom: const.  $E$  rescaled to const  $\Psi_S$**

**and additional const  $\Psi_S$  validation data**

Thus, we propose the extended display reflection model, which is an evolution of Kelley's original model:

$$L_{Ref} = \frac{\rho + R_{Haze}(\Psi_S)}{\pi} E + [\xi + R_{Diff}(\Psi_S)]L_S \quad (5)$$

**7. Summary, impact, and outlook**

We validated an ILMD-based measurement setup for its capability to separate the specular and Lambertian reflection components by comparing it to established setups. Then we used this approach to additionally separate and analyze the diffractive component of display reflection. Measurements using a VAS showed that the diffraction scales with the light source luminance and that it is a function of the light source angular subtense. Although unsurprising, this combination is unique among the reflection components. Thus, an extension of Kelley's original three-component model is reasonable.

The example data also shows that existing measurement principles can be affected by diffraction. For three out of five DUTs reflection profiles presented in this paper (Figure 2, 3 and 6), the measurement of the Lambertian component at the established 45/0 geometry would have been massively impacted by diffraction, leading to erroneous reflection data and models for these DUTs. However, ILMD-based reflection metrology, such as the conoscopic approach – or the PSF to BRFD approach [8] – enables the generation of more precise reflection models in a reasonable amount of time.

Still, there are challenges to overcome. At viewing angles where haze is present, our analysis cannot be used to isolate the diffractive components. Another relevant topic for future consideration is the efficient measurement of data that allows generating colorimetric diffraction models.

**8. References**

1. Kwon, S., et. al. (2024), P-266: Late-News Poster: Quality Assessment Towards Reflective Pattern Based on Diffraction Appearance. SID Symposium Digest of Technical Papers, 55: 2256-2259.
2. CIE 244:2021, Characterization of Imaging Luminance Measurement Devices (ILMDs), 2021.
3. Penczek, J. (2024), 74-3: Regular Reflectance and Transmittance Measured by the Annulus Source Method. SID Symposium Digest of Technical Papers, 55: 1015-1018.
4. E. F. Kelley et. al. "Display reflectance model based on the BRDF," Displays, vol. 19, pp. 27-34, 1998.
5. Penczek, J., et. al. (2022), 39-2: Evaluating the Components of Reflected Glare in Displays. SID Symposium Digest of Technical Papers, 53: 489-492.
6. Hertel, D., et. al. (2020), 64-1: Separating Specular Reflection from Diffuse Haze for ePa-per Using the Extended Variable-Aperture Source Method. SID Symposium Digest of Technical Papers, 51: 949-952.
7. Voelz, A., et. al., Optimized Workflow for Fast and Precise ISO 15008 Contrast Evaluation under Ambient Light, to be published in Information Display (2025)
8. Becker, M.E. (2004), 13.1: Measurement and Evaluation of Display Scattering. SID Symposium Digest of Technical Papers, 35: 184-187. <https://doi.org/10.1889/1.1821383>